SCIENCE CHINA

Technological Sciences



Article

November 2021 Vol.64 No.11: 2408–2414 https://doi.org/10.1007/s11431-021-1899-9

Highly sensitive piezoresistive pressure sensors based on laser-induced graphene with molybdenum disulfide nanoparticles

HAO DaPeng^{1,2†}, YANG RuoXi^{2,3†}, YI Ning⁴ & CHENG HuanYu^{2,4*}

¹ School of Science, Xi'an Aeronautical University, Xi'an 710077, China;

Received May 27, 2021; accepted July 19, 2021; published online August 28, 2021

Wearable pressure sensors have drawn significant attention because of their extensive applications in motion detection, tactile sensing, and health monitoring. However, the complex manufacturing process and high cost of active materials make low-cost, large-scale production elusive. In this work, we report a flexible piezoresistive pressure sensor assembled with two 3D laser-induced graphene (LIG) foam electrodes on a polyimide thin film from a simple laser scribing process in the ambient environment. The design of the air gap between the two foam electrodes allows the sensor to showcase a low limit of detection of 0.274 Pa, which provides favorable sensing performance in motion detection and wrist pulse monitoring. The addition of spherical MoS₂ nanoparticles between the two foam electrodes further enhances the sensitivity to 88 kPa⁻¹ and increases the sensing range to significantly outperform the previous literature reports. The demonstrated LIG pressure sensors also exhibit fast response/recovery rates and excellent durability/repeatability.

piezoresistive pressure sensor, laser-induced graphene foam, molybdenum disulfide nanoparticles, health monitoring

Citation: Hao D P, Yang R X, Yi N, et al. Highly sensitive piezoresistive pressure sensors based on laser-induced graphene with molybdenum disulfide nanoparticles. Sci China Tech Sci, 2021, 64: 2408–2414, https://doi.org/10.1007/s11431-021-1899-9

1 Introduction

The emerging soft, stretchable, bio-integrated electronics start to gain popularity due to their unique advantage to continuously monitor the clinically relevant physiological parameters from the skin surface to inform health conditions [1–3]. In particular, wearable pressure sensors have been extensively studied for motion detection [4], tactile sensing [5], human-computer interface [6], and health monitoring [7,8]. Various novel materials and nanostructures have been exploited in wearable pressure sensors [9–13]. Compared with capacitive [14], piezoelectric [15], and triboelectric [16], the piezoresistive [17] pressure sensors are most widely

used because of their simple data acquisition setup and low-cost characteristic. However, piezoresistance pressure sensors often suffer from low sensitivity and slow response/recovery rates because of the high modulus and viscoelasticity in the pressure-sensing active materials [18]. The efforts to enhance the sensitivity have resulted in the exploration of various structures for rapid changes in conductive pathways. The commonly used micro-/nano-structures include pyramids [19–22], microdomes [11,21], micropillars [23], multilayered structures [24], or porous structures [25]. However, the preparation of these structures is often associated with increased complexity and high cost. Moreover, the sensing range is relatively small because the conductive pathways quickly saturate with the increasing applied pressure.

² Department of Engineering Science and Mechanics, The Pennsylvania State University, University Park, State College PA 16802, USA; ³ School of Mechanical Engineering, Hebei University of Technology, Tianjin 300401, China;

⁴ Department of Materials Science and Engineering, The Pennsylvania State University, University Park, State College PA 16802, USA

[†]These authors contributed equally to this work.

^{*}Corresponding author (email: Huanyu.Cheng@psu.edu)

In addition to the innovative structural designs, advanced novel materials with excellent electrical performance and microstructure (e.g., wrinkled graphene film [24], nanowire [26], and nanoparticles such as a sea-urchin shape [27]) have also been reported to be beneficial for constituting the conductive network under pressing and improving sensitivity. Among these materials, graphene has been regarded as the ideal material for the piezoresistive pressure sensor due to its remarkable mechanical strength, flexibility, and electrical conductivity. Interestingly, the laser-induced graphene (LIG) foam from commercially available polyimide (PI) thin film [28] combines the few-layered graphene materials with the 3D porous foam structures, creating applications in microsupercapacitors [29,30], stretchable gas sensors [31], and antennas/rectennas [32]. In addition to PI [33,34], graphene oxide (GO) [35,36] and polydimethylsiloxane (PDMS) [37] can also be converted into LIG foam. Although LIG foam transferred to elastic PDMS [33] or polyurethane (PU) [34] has been explored to improve the flexibility and the sensitivity (i.e., changes in the resistance) upon pressure loading, the transfer process often damages the surface microstructure of the LIG, compromising its capability to sense the small pressure.

In this work, we directly assemble two LIG foam elec-

trodes on the flexible PI thin films that are separated to provide an air gap for achieving a lower limit of detection of 0.274 Pa. Because the deformation of soft materials results in quick saturation of the conductive pathways, the pressure sensor with high sensitivity is often associated with a small sensing range [12,38,39]. To address this challenge, we further explore spherical MoS₂ nanoparticles (NPs) between two LIG foam electrodes to increase the mechanical robustness of the pressure sensor for increased sensing range. Because of the spherical shape of the MoS₂ NPs, their rolling and lateral motions upon pressure loading also allow the sensor to exhibit a high sensitivity of 88 kPa⁻¹ for simultaneously improved sensitivity and sensing range. Moreover, the flexible LIG pressure sensor also showcases fast response/recovery rates and high stability over 9000 loading/ unloading cycles.

2 Results and discussion

2.1 Fabrication of the LIG pressure sensor

The fabrication of the LIG pressure sensor combines the 3D LIG foam with the spherical MoS_2 NPs (Figure 1(a)). Briefly, the PI film with a thickness of 25 μ m on the glass

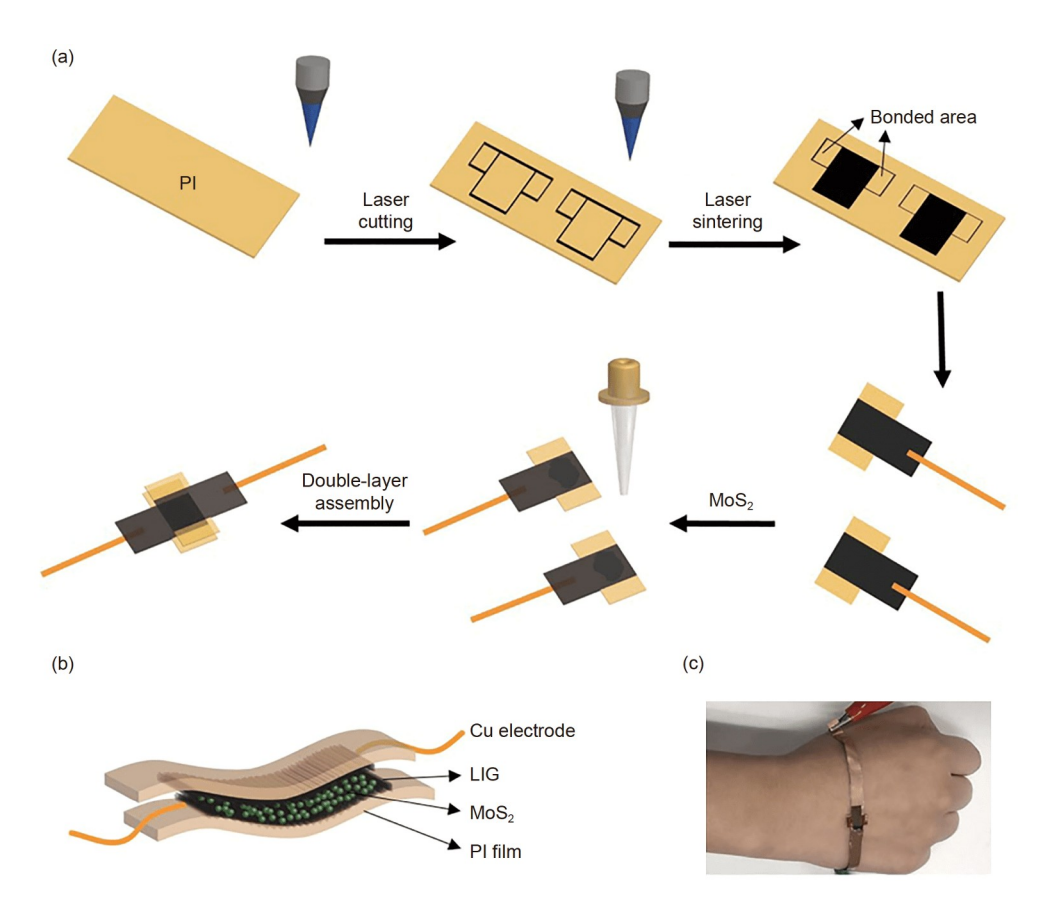


Figure 1 (Color online) Schematic of the fabrication process and the photograph of the resulting LIG pressure sensor. (a) Schematic to show the fabrication process of the LIG pressure sensor; (b) the schematic diagram of the LIG pressure sensor with the layout information; (c) photograph of the LIG pressure sensor pliably conformed on the skin surface of the hand.

slide is patterned into sensing and bonding regions designed by CorelDRAW. The profile of the sensor is scribed by a CO₂ laser system with low power (8%) and high speed (90%), and the sensing area is sintered by the same CO₂ laser system with 35% power and 40% speed to yield 3D porous LIG foam; then, the fabricated sensing unit is connected to copper electrodes by Ag paster. Next, the MoS₂ NP solution synthesized by a solvothermal method [40] is drop-cast in the sensing region, followed by solvent evaporation in the oven at a temperature of 60°C for 1 h. The MoS₂ NP solution is successively added onto the surface of LIG in a step of 1 uL to avoid accumulation (Figure S1). After applying the double-sided tape with a thickness of 40 µm at the bonding region, flipping over one LIG foam to assemble onto the other LIG foam completes the fabrication of the piezoresistive LIG pressure sensor. Though the manual assembly process introduces slight variations in device performance, the issue could be addressed by exploring the motorized equipment to aid the alignment and assembly. The resulting flexible LIG pressure sensor (Figure 1(b)) can easily attach to the skin surface through an adhesive layer, which demonstrates a robust adhesion strengthen even upon mechanical deformations (e.g., holding a fist, Figure 1(c)).

2.2 Demonstration of the LIG pressure sensors without MoS_2

The few-layered [31,32], 3D porous LIG foams (Figure 2(a)) with thorn-like structures (Figure 2(b)) provide the conductive pathway between the top and bottom layers in the piezoresistance LIG pressure sensor. The initial relative position of the two electrodes separated by a small gap is provided by the double-sided adhesive tape changes upon the pressure loading to result in more conductive pathways and then increased conductance of the LIG sensor (Figure 2(c)). The LIG pressure sensor with the air gap has fewer conductive pathways, allowing the sensor to more sensitively detect the tiny pressure change. Consequently, the LIG

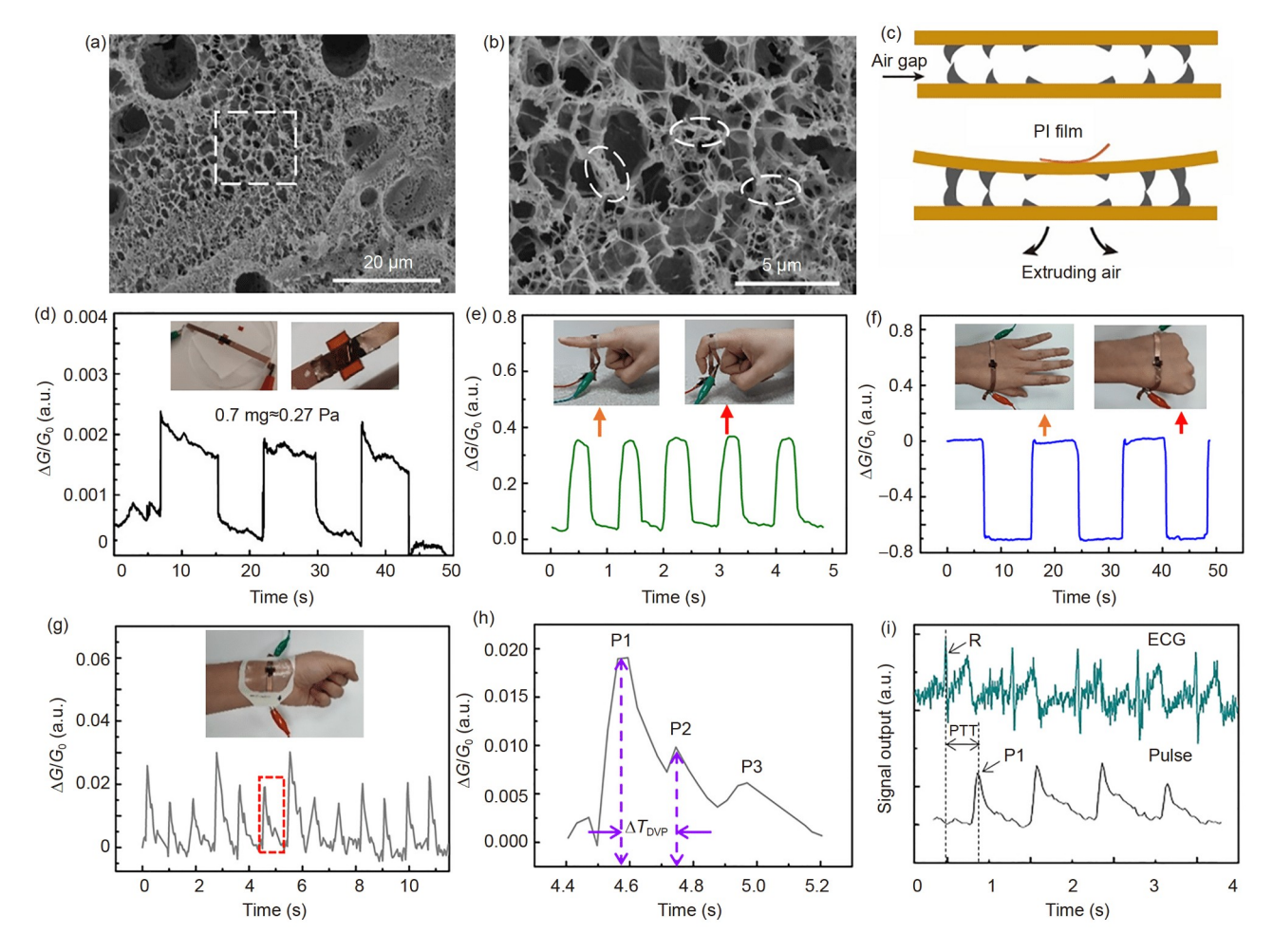


Figure 2 (Color online) The application demonstration of the LIG pressure sensor. (a) Scanning electron microscopy (SEM) images of the LIG with the area in the dashed box enlarged in (b) to show the thorn-like structures (marked); (c) schematic to show the LIG sensor for small pressure measurement; (d) repeated tiny pressure loading with PI film; (e) and (f) LIG pressure sensor to detect (e) finger and (f) hand movements; (g) real-time responses of the LIG pressure sensor for pulse monitoring; (h) the enlarged view of the dashed box in (g) shows the three characteristic peaks with the time difference between the first two peaks labeled; (i) schematic to show the principle that uses the pulse profile and ECG for blood pressure measurements.

pressure sensor with the air gap exhibits a low limit of detection to be capable of detecting a pressure of 0.274 Pa (or a force of 0.7 mg) when a PI film is placed on the surface of the sensor (Figure 2(d)). The demonstrated low limit of detection with a stable and repeatable sensor response is smaller than the previously reported LIG and other nanostructured pressure sensors [24,34,36–38,41].

Because the thin LIG pressure sensor features favorable mechanics, which allows it to be attached to various curvilinear surfaces (e.g., finger and back of the hand) of the human body for human motion detection. For instance, the attachment of the LIG pressure sensor on the index finger easily detects the bending motions (Figure 2(e)). The bending deformation brings the lower LIG foam electrode closer to the upper one to increase the conductive pathways and increase the conductance. When the flexible LIG pressure sensor is attached to the back of the hand, holding a fist stretches the lower LIG foam electrode to increase the gap between two LIG electrodes to result in decreased resistance (Figure 2(f)). The above results indicate that the flexible LIG pressure sensor can distinguish the bending from stretching motion, as the conductance increases in the former but decreases in the latter.

As another representative demonstration, the flexible LIG pressure sensor attached to the wrist by a transparent medical tape measures the pulse that generates pressure on the sensor in real-time. The pulse measurements from a healthy human subject show a resting heart rate of ca. 68 beats min⁻¹ (Figure 2(g)), which agrees with the value from manual counting. Moreover, the measured pulse profiles clearly identify three distinct characteristic peaks, i.e., percussion wave (P1), tidal wave (P2), and diastolic wave (P3) (Figure 2(h)).

These characteristic peaks are lost in the measurements from many pressure sensors reported previously [12,42–44]. The ratio (i.e., augmentation index of radial artery) [45] and time difference ($\Delta T_{\rm DVP}$) [46] of P1 and P2 waves that are related to arterial stiffness could provide significant insights into cardiac health. Additionally, the pulse profiles can be combined with the simultaneous electrocardiogram (ECG) measurements (Figure 2(i)) to yield cuffless measurements of the arterial blood pressure using a pulse transit time method, as another essential physiological parameter for health monitoring.

2.3 Enhanced LIG pressure sensors with MoS₂ NPs

Although the above intrinsic flexible LIG or other nanostructured pressure sensors can detect the pressure, the varied conducting pathways quickly saturate because of the easy deformation of the soft materials upon pressure loading. Therefore, most of the previous nanostructured pressure sensors exhibit a low sensitivity and narrow sensing range. This study further introduces previously reported spherical semiconducting MoS₂ NPs [31] into the 3D porous LIG foams to increase their mechanical strength against pressure loading (Figures 3(a) and 4(a)). The spherical shape of the non-conductive MoS₂ NPs also allows them to displace upon pressure loading for enhanced sensing range. The spherical shape of the MoS₂ NPs also allows them to displace upon pressure loading for enhanced sensing range. Compared to the intrinsic LIG pressure sensor, the LIG pressure sensor with the spherical MoS₂ NPs shows a much large increase in the initial resistance from ca. 110 Ω to 10 k Ω . Because of the rolling and lateral movements of the spherical MoS₂ NPs, the

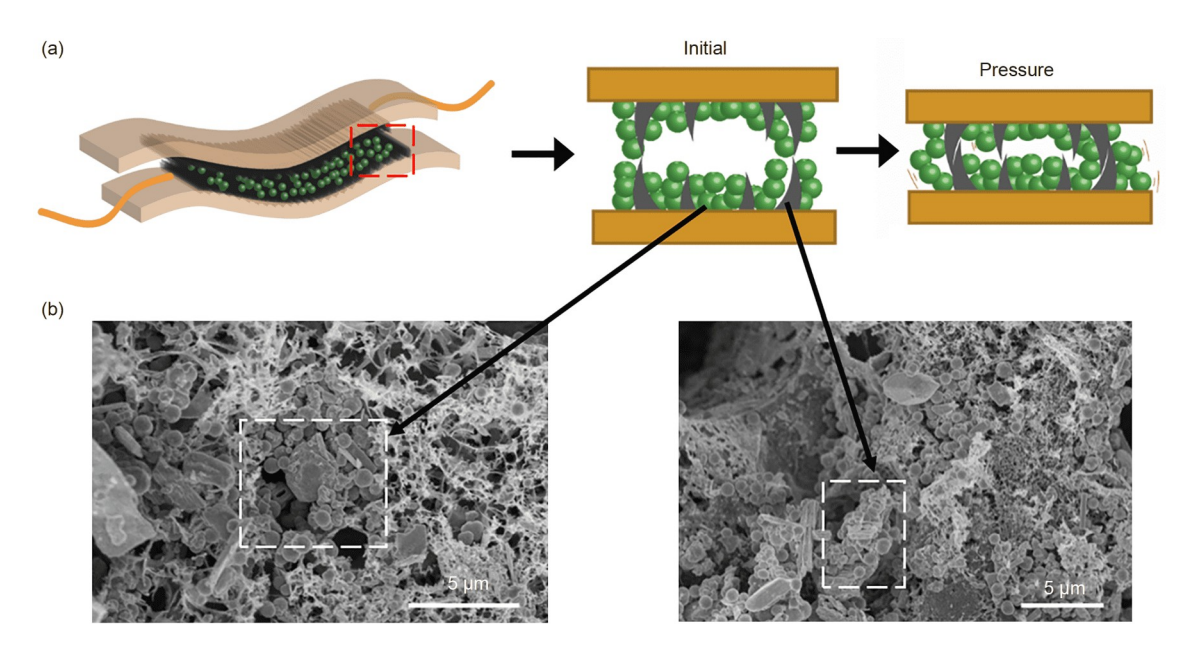


Figure 3 (Color online) The schematic and SEM images of the LIG pressure sensor with MoS_2 . (a) LIG pressure sensor with MoS_2 fillers before and after pressure loading; (b) SEM images of porous LIG foams filled with MoS_2 (left) and thorns surrounded by MoS_2 (right).

large initial resistance rapidly reduces to result in increased sensitivity in the pressure sensor.

The sensitivity (S) of the flexible LIG pressure sensor with the spherical MoS₂ NPs is calculated from the measured relative conductance change ($\Delta G/G_0$ with G_0 as the initial conductance) versus the applied pressure (P) as $S=(\Delta G/G_0)/P$. Because of the added MoS₂ NPs, the sensitivity of 3.29 kPa⁻¹ is relatively small in the lower pressure range (i.e., <0.94 kPa) (Figure 4(a)). However, as the applied pressure exceeds the critical value to displace the MoS₂ NPs, the pressure sensor exhibits a significantly higher sensitivity of 88 kPa⁻¹ in the range from 0.94 to 1.44 kPa. As the increased conductive pathways gradually saturate with the increasing applied pressure, the sensitivity decreases to 6 kPa⁻¹ in the range from 1.44 to 6.25 kPa and then decreases to 0.29 kPa⁻¹ for the pressure over 6.25 kPa, which is consistent with literature reports. Compared with the previously reported graphene-based or nanostructured pressure sensors in the range of [0.94, 6.25] kPa [12,41,47-56], the demonstrated LIG pressure sensor with MoS₂ NPs exhibits enhanced sensitivity and linear range (Figure 4(d), Table S1). Because the enhanced performance is attributed to spherical MoS₂ NPs, the enhancement depends on the relative quantity of the MoS₂ NPs. The low concentration of MoS₂ results in most of the MoS_2 NPs distributing inside porous LIG foams, whereas the excess MoS_2 would cover and compromise the porous structure in the 3D LIG foams. Therefore, an optimal concentration of the MoS_2 NP solution exists, which is found to be 25 μL in the range from 0 to 40 μL for the LIG pressure sensor with an area of 5 mm×5 mm (Figure S2).

The LIG pressure sensor with MoS₂ NPs also exhibits reasonably good repeatability, which confirmed over 9000 loadings and unloading cycles for an applied pressure of 1 kPa (Figure 4(b)). The almost identical relative resistance changes $(\Delta G/G_0)$ at the beginning ten cycles and the last ten cycles showcase the excellent durability and reliability of the sensor performance. Because real-time pressure monitoring requires fast sensor response, fast response/recovery rates are demonstrated with rapid finger pressure applied to the sensor. Although the measured results indicate a response and recovery time of \sim 60 ms for the LIG pressure sensor (Figure 4(c)), the actual response/recovery rates could be even faster because the current measurements are limited by the sampling rate of the equipment. Nevertheless, the response/recovery rates are already more than three orders of magnitude faster than several previous reports [4,24,51]. The fast rates are likely attributed to the quick movements of the MoS₂ NPs in a spherical shape.

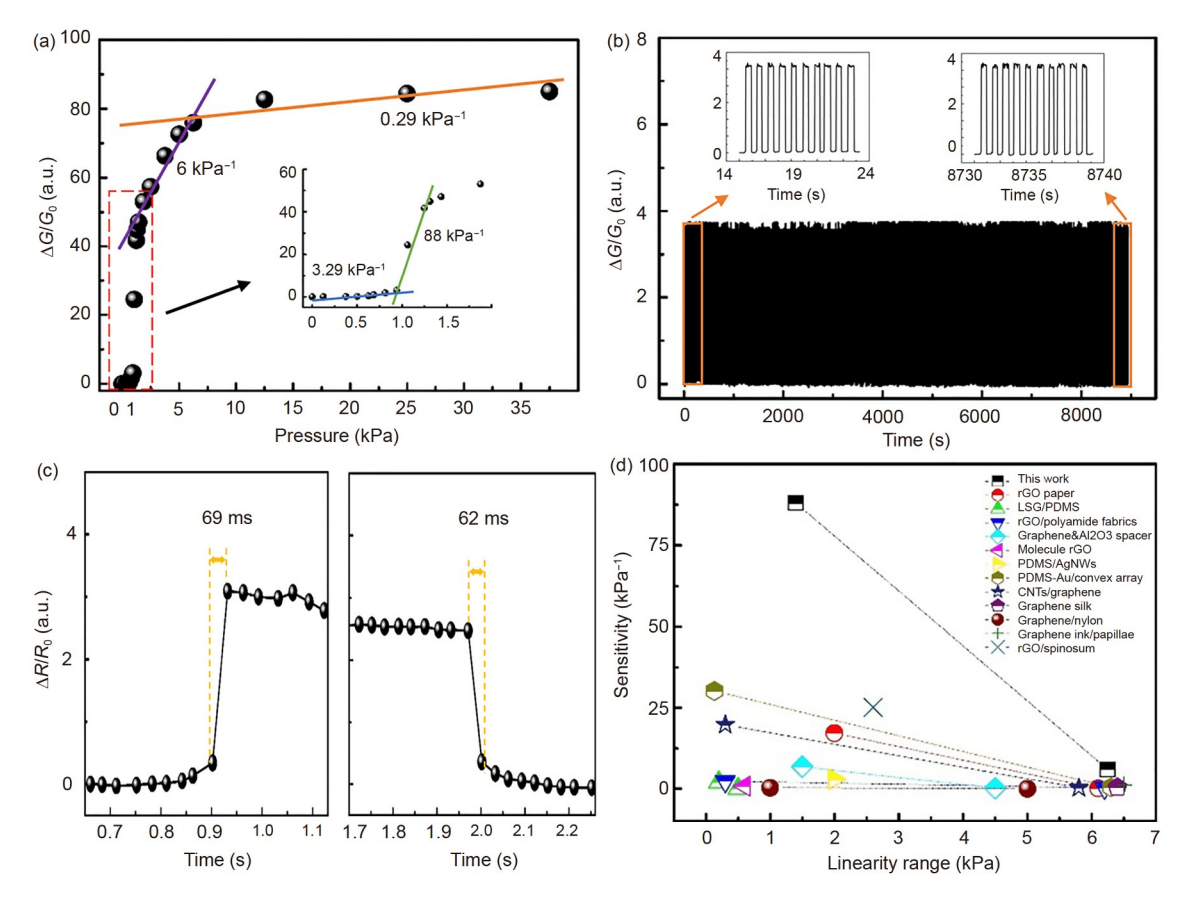


Figure 4 (Color online) Electromechanical characterization of the LIG pressure sensor with MoS₂. (a) The change in the normalized relative conductance with the applied pressure; (b) repeatability test for 9000 pressuring-releasing cycles; (c) response and recovery time of the LIG pressure sensor; (d) comparison of the sensitivity and linear range between our work and previously reported pressure sensors.

3 Conclusion

This work develops a low-cost fabrication of flexible piezoresistive LIG pressure sensors for wearable applications. The design of the air gap between two LIG foam electrodes provides the sensor with a low limit of detection of 0.274 Pa, which allows the sensor to measure human motions and waist pulse in real-time. Furthermore, the addition of MoS₂ NPs between the two LIG foam electrodes results in enhanced sensitivity and sensing range, which significantly outperforms the previous literature reports. The demonstrated flexible LIG pressure sensors have shown great potential to complement existing wearable devices for healthcare monitoring.

YANG RuoXi acknowledges the support from the Joint Doctoral Training Foundation of HEBUT. CHENG HuanYu would like to acknowledge the supports from the National Natural Science Foundation of China (Grant No. ECCS-1933072), the National Heart, Lung, and Blood Institute of the National Institutes of Health (Grant No. R61HL154215), and the Penn State University (Center for Security Research and Education, Center for Biodevices, and College of Engineering Multidisciplinary Seed Grants).

Supporting Information

The supporting information is available online at tech.scichina.com and link.springer.com. The supporting materials are published as submitted, without typesetting or editing. The responsibility for scientific accuracy and content remains entirely with the authors.

- 1 Trung T Q, Dang T M L, Ramasundaram S, et al. A stretchable straininsensitive temperature sensor based on free-standing elastomeric composite fibers for on-body monitoring of skin temperature. ACS Appl Mater Interfaces, 2019, 11: 2317–2327
- 2 Yin B, Liu X, Gao H, et al. Bioinspired and bristled microparticles for ultrasensitive pressure and strain sensors. Nat Commun, 2018, 9: 5161
- 3 Zhao Y, Zhai Q, Dong D, et al. Highly stretchable and strain-insensitive fiber-based wearable electrochemical biosensor to monitor glucose in the sweat. Anal Chem, 2019, 91: 6569–6576
- 4 Tao L Q, Zhang K N, Tian H, et al. Graphene-paper pressure sensor for detecting human motions. ACS Nano, 2017, 11: 8790–8795
- 5 Miao P, Wang J, Zhang C, et al. Graphene nanostructure-based tactile sensors for electronic skin applications. Nano-Micro Lett, 2019, 11: 1– 37
- 6 Jeon G J, Yeom H I, Jin T, et al. A highly sensitive, stable, scalable pressure sensor based on a facile baking-inspired foaming process for a human-computer interface. J Mater Chem C, 2020, 8: 4271–4278
- 7 Lou Z, Chen S, Wang L, et al. An ultra-sensitive and rapid response speed graphene pressure sensors for electronic skin and health monitoring. Nano Energy, 2016, 23: 7–14
- 8 Han Z, Cheng Z, Chen Y, et al. Fabrication of highly pressure-sensitive, hydrophobic, and flexible 3D carbon nanofiber networks by electrospinning for human physiological signal monitoring. Nanoscale, 2019, 11: 5942–5950
- 9 Zhu B, Ling Y, Yap L W, et al. Hierarchically structured vertical gold nanowire array-based wearable pressure sensors for wireless health monitoring. ACS Appl Mater Interfaces, 2019, 11: 29014–29021
- 10 Kim S, Amjadi M, Lee T I, et al. Wearable, ultrawide-range, and bending-insensitive pressure sensor based on carbon nanotube network-coated porous elastomer sponges for human interface and healthcare devices. ACS Appl Mater Interfaces, 2019, 11: 23639– 23648

- 11 Yu G H, Hu J D, Tan J P, et al. A wearable pressure sensor based on ultra-violet/ozone microstructured carbon nanotube/polydimethylsiloxane arrays for electronic skins. Nanotechnology, 2018, 29: 115502.
- 12 Pang Y, Zhang K, Yang Z, et al. Epidermis microstructure inspired graphene pressure sensor with random distributed spinosum for high sensitivity and large linearity. ACS Nano, 2018, 12: 2346–2354
- Han Z, Li H, Xiao J, et al. Ultralow-cost, highly sensitive, and flexible pressure sensors based on carbon black and airlaid paper for wearable electronics. ACS Appl Mater Interfaces, 2019, 11: 33370–33379
- 14 Yang J, Luo S, Zhou X, et al. Flexible, tunable, and ultrasensitive capacitive pressure sensor with microconformal graphene electrodes. ACS Appl Mater Interfaces, 2019, 11: 14997–15006
- 15 Yang Y, Pan H, Xie G, et al. Flexible piezoelectric pressure sensor based on polydopamine-modified BaTiO₃/PVDF composite film for human motion monitoring. Sens Actuat A-Phys, 2020, 301: 111789
- 16 Das P S, Chhetry A, Maharjan P, et al. A laser ablated graphene-based flexible self-powered pressure sensor for human gestures and finger pulse monitoring. Nano Res, 2019, 12: 1789–1795
- 17 Park S J, Kim J, Chu M, et al. Flexible piezoresistive pressure sensor using wrinkled carbon nanotube thin films for human physiological signals. Adv Mater Technol, 2018, 3: 1700158
- 18 Ruth S R A, Feig V R, Tran H, et al. Microengineering pressure sensor active layers for improved performance. Adv Funct Mater, 2020, 30: 2003491
- Huang Z, Gao M, Yan Z, et al. Pyramid microstructure with single walled carbon nanotubes for flexible and transparent micro-pressure sensor with ultra-high sensitivity. Sens Actuat A-Phys, 2017, 266: 345-351
- 20 Li H, Wu K, Xu Z, et al. Ultrahigh-sensitivity piezoresistive pressure sensors for detection of tiny pressure. ACS Appl Mater Interfaces, 2018, 10: 20826–20834
- 21 Peng S, Blanloeuil P, Wu S, et al. Rational design of ultrasensitive pressure sensors by tailoring microscopic features. Adv Mater Interfaces, 2018, 5: 1800403
- 22 Li G, Chen D, Li C, et al. Engineered microstructure derived hierarchical deformation of flexible pressure sensor induces a supersensitive piezoresistive property in broad pressure range. Adv Sci, 2020, 7: 2000154
- 23 Cheng L, Qian W, Wei L, et al. A highly sensitive piezoresistive sensor with interlocked graphene microarrays for meticulous monitoring of human motions. J Mater Chem C, 2020, 8: 11525–11531
- 24 Liu W, Liu N, Yue Y, et al. Piezoresistive pressure sensor based on synergistical innerconnect polyvinyl alcohol nanowires/wrinkled graphene film. Small, 2018, 14: 1704149
- 25 Yang J C, Kim J O, Oh J, et al. Microstructured porous pyramid-based ultrahigh sensitive pressure sensor insensitive to strain and temperature. ACS Appl Mater Interfaces, 2019, 11: 19472–19480
- 26 Xu X, Wang R, Nie P et al. Copper nanowire-based aerogel with tunable pore structure and its application as flexible pressure sensor. ACS Appl Mater Interfaces, 2017, 9: 14273–14280
- 27 Lee D, Lee H, Jeong Y, et al. Highly sensitive, transparent, and durable pressure sensors based on sea-urchin shaped metal nanoparticles. Adv Mater, 2016, 28: 9364–9369
- 28 Lin J, Peng Z W, Liu Y Y, et al. Laser-induced porous graphene films from commercial polymers. Nat Commun, 2014, 5: 5714
- 29 Ye R, James D K, Tour J M. Laser-induced graphene: From discovery to translation. Adv Mater, 2019, 31: 1803621
- 30 Zhang C, Peng Z, Huang C, et al. High-energy all-in-one stretchable micro-supercapacitor arrays based on 3D laser-induced graphene foams decorated with mesoporous ZnP nanosheets for self-powered stretchable systems. Nano Energy, 2021, 81: 105609
- 31 Yang L, Yi N, Zhu J, et al. Novel gas sensing platform based on a stretchable laser-induced graphene pattern with self-heating capabilities. J Mater Chem A, 2020, 8: 6487–6500
- 32 Zhu J, Hu Z, Song C, et al. Stretchable wideband dipole antennas and rectennas for RF energy harvesting. Mater Today Phys, 2021, 18:

- 100377
- 33 Wakabayashi S, Arie T, Akita S, et al. Very thin, macroscale, flexible, tactile pressure sensor sheet. ACS Omega, 2020, 5: 17721–17725
- 34 Tian Q, Yan W, Li Y, et al. Bean pod-inspired ultrasensitive and self-healing pressure sensor based on laser-induced graphene and poly-styrene microsphere sandwiched structure. ACS Appl Mater Interfaces, 2020, 12: 9710–9717
- Tian H, Shu Y, Wang X F, et al. A graphene-based resistive pressure sensor with record-high sensitivity in a wide pressure range. Sci Rep, 2015, 5: 8603
- 36 Zhu Y, Li J, Cai H, et al. Highly sensitive and skin-like pressure sensor based on asymmetric double-layered structures of reduced graphite oxide. Sens Actuat B-Chem, 2018, 255: 1262–1267
- 37 Zhu Y S, Cai H B, Ding H Y, et al. Fabrication of low-cost and highly sensitive graphene-based pressure sensors by direct laser scribing polydimethylsiloxane. ACS Appl Mater Interfaces, 2019, 11: 6195– 6200
- 38 Luo Y, Shao J, Chen S, et al. Flexible capacitive pressure sensor enhanced by tilted micropillar arrays. ACS Appl Mater Interfaces, 2019, 11: 17796–17803
- 39 Han S, Liu C, Huang Z, et al. High-performance pressure sensors based on 3d microstructure fabricated by a facile transfer technology. Adv Mater Technol, 2019, 4: 1800640
- 40 Yi N, Cheng Z, Li H, et al. Stretchable, ultrasensitive, and low-temperature NO₂ sensors based on MoS₂@rGO nanocomposites. Mater Today Phys, 2020, 15: 100265
- 41 Huang C B, Witomska S, Aliprandi A, et al. Molecule-graphene hybrid materials with tunable mechanoresponse: Highly sensitive pressure sensors for health monitoring. Adv Mater, 2019, 31: 1804600
- 42 Guo S Z, Qiu K, Meng F, et al. 3D printed stretchable tactile sensors. Adv Mater, 2017, 29: 1701218
- 43 Yang J, Ye Y, Li X, et al. Flexible, conductive, and highly pressuresensitive graphene-polyimide foam for pressure sensor application. Compos Sci Tech, 2018, 164: 187–194
- 44 Chen Z, Wang Z, Li X, et al. Flexible piezoelectric-induced pressure sensors for static measurements based on nanowires/graphene heterostructures. ACS Nano, 2017, 11: 4507–4513
- 45 Munir S, Jiang B, Guilcher A, et al. Exercise reduces arterial pressure

- augmentation through vasodilation of muscular arteries in humans. Am J Physiol-Heart Circulatory Physiol, 2008, 294: H1645–H1650
- 46 Chen C H, Ting C T, Nussbacher A, et al. Validation of carotid artery tonometry as a means of estimating augmentation index of ascending aortic pressure. Hypertension, 1996, 27: 168–175
- 47 Joo Y, Byun J, Seong N, et al. Silver nanowire-embedded PDMS with a multiscale structure for a highly sensitive and robust flexible pressure sensor. Nanoscale, 2015, 7: 6208–6215
- 48 Shuai X, Zhu P, Zeng W, et al. Highly sensitive flexible pressure sensor based on silver nanowires-embedded polydimethylsiloxane electrode with microarray structure. ACS Appl Mater Interfaces, 2017, 9: 26314–26324
- 49 Yin F, Yang J, Peng H, et al. Flexible and highly sensitive artificial electronic skin based on graphene/polyamide interlocking fabric. J Mater Chem C, 2018, 6: 6840–6846
- 50 Chen W, Gui X, Liang B, et al. Structural engineering for high sensitivity, ultrathin pressure sensors based on wrinkled graphene and anodic aluminum oxide membrane. ACS Appl Mater Interfaces, 2017, 9: 24111–24117
- 51 Ma L, Shuai X, Hu Y, et al. A highly sensitive and flexible capacitive pressure sensor based on a micro-arrayed polydimethylsiloxane dielectric layer. J Mater Chem C, 2018, 6: 13232–13240
- 52 Xiong Y, Shen Y, Tian L, et al. A flexible, ultra-highly sensitive and stable capacitive pressure sensor with convex microarrays for motion and health monitoring. Nano Energy, 2020, 70: 104436
- 53 Jian M, Xia K, Wang Q, et al. Flexible and highly sensitive pressure sensors based on bionic hierarchical structures. Adv Funct Mater, 2017, 27: 1606066
- 54 Liu Y, Tao L Q, Wang D Y, et al. Flexible, highly sensitive pressure sensor with a wide range based on graphene-silk network structure. Appl Phys Lett, 2017, 110: 123508
- 55 He Z, Chen W, Liang B, et al. Capacitive pressure sensor with high sensitivity and fast response to dynamic interaction based on graphene and porous nylon networks. ACS Appl Mater Interfaces, 2018, 10: 12816–12823
- 56 Shi J, Wang L, Dai Z, et al. Multiscale hierarchical design of a flexible piezoresistive pressure sensor with high sensitivity and wide linearity range. Small, 2018, 14: e1800819